Aalborg Universitet

Radiation Pattern Reconfigurable Mm-Wave Bow-Tie Array Integrated with PIFA Antenna

Cano, Rocio Rodriguez; Zhang, Shuai; Pedersen, Gert Frølund

Published in:
2019 IEEE 90th Vehicular Technology Conference (VTC2019-Fall)

DOI (link to publication from Publisher):
10.1109/VTCFall.2019.8891496

Publication date:
2019

Document Version
Accepted author manuscript, peer reviewed version

Citation for published version (APA):
Cano, R. R., Zhang, S., & Pedersen, G. F. (2019). Radiation Pattern Reconfigurable Mm-Wave Bow-Tie Array Integrated with PIFA Antenna. In *2019 IEEE 90th Vehicular Technology Conference (VTC2019-Fall)* [8891496] IEEE. I E E E V T S Vehicular Technology Conference. Proceedings https://doi.org/10.1109/VTCFall.2019.8891496

Radiation Pattern Reconfigurable Mm-Wave Bow-Tie Array Integrated with PIFA Antenna

Rocío Rodríguez-Cano, Shuai Zhang, Gert F. Pedersen
Antenna, Propagation and Mm-Wave Systems Section (APMS), Department of Electronic Systems,
Aalborg University, Aalborg, Denmark
{*rrc, sz, gfp*}*@es.aau.dk*

***Abstract*—In this paper, a millimeter-wave (mm-wave) bow-tie antenna array is proposed to be integrated with a low-frequency Planar Inverted F-Antenna (PIFA) at the top edge of a handset. A layer of grating strips with pin diodes is added between the low and high-frequency antennas to provide reconfigurable radiation patterns. The proposed 5G array is matched from 24-30 GHz and can steer the beam in both configurations with a realized gain higher than 8 dBi in the broadside case, and more than 6 dBi when the radiation pattern is endfire.**

***Index Terms*—5G mobile communication, antenna array, radiation pattern, reconfigurable**

I. INTRODUCTION

The fifth generation of mobile communications (5G) includes some frequency ranges in the millimeter-wave (mm-wave) band to alleviate the saturated spectrum under 3 GHz [1]. High-gain antenna systems are required to compensate higher propagation losses [2], [3]. Due to the limited space available in mobile terminals, the placement of the mm-wave arrays can be challenging.

One solution to save space consist of integrating the 5G array with the antennas from the former generations. However, having metallic structures in the same direction as the main beam of a planar endfire mm-wave antenna can partially or totally block the beam of the 5G antenna. Several solutions have been proposed in literature to reduce the blockage. In [4], a Vivaldi array has been integrated with the metal case of the phone, that acts as the low-frequency antenna. Two layers of metal strips are placed at both sides of the frame and are illuminated by the coupling from the reflections on the frame. The radiation from the two layers, adds in phase in the far-field. In [5], a window has been etched from the frame to include the mm-wave module. The sub-6 GHz frame antenna and the mm-wave array are co-designed. In [6], a folded-dipole array is combined with a dual-band Planar Inverted F-Antenna (PIFA). In order to overcome the blockage of the PIFA, anti-reflecting coating is introduced at a quarter wavelength to make the reflections from the PIFA and the coating cancel out. Several pattern reconfigurable antennas have been proposed in literature for 5G. In [7], a radiation pattern reconfigurable antenna is proposed with three switchable modes. However the structure is composed of three stacked layers, which complicated the fabrication process. In [8], a 3-dimensional reconfigurable array for base station that allows to cover sectors of 90° is presented.

In this paper, a mm-wave bow-tie array is integrated with a low-frequency PIFA antenna. The diodes introduced between the layer of grating strips allow the reconfigurability of the radiation pattern.

II. ANTENNA DESIGN

The mm-wave array is composed of 4 antipodal bow-tie antenna elements, as represented in Fig. 1 (a). A layer of anti-reflective grating strips is placed between the array and the metallic branch of the PIFA. The PIFA serves as sub-3 GHz antenna and occupies all the width of the handset. Diodes are placed between the grating strips to provide the reconfigurability functionality of the radiation pattern, as shown in Fig. 1 (b). The number of grating strips and diodes needs to be larger than the array aperture to cover the maximum beam-steering angle. Otherwise the radiation pattern would be degraded. When the pin diodes are on, the equivalent circuit corresponds to a series resistance and inductance, which blocks the radiation from the antenna resulting in broadside radiation pattern. If the pin diodes are off, the model corresponds to a capacitance in series with an inductance, allowing the radiation pass between the strips and endfire radiation pattern is obtained. It is required that all the diodes are on or off, respectively, to not degrade the radiation pattern. As explained in [6], the reflections from the grating strips and the low-frequency antenna are out of phase, therefore they cancel out. For convenience, we refer to endfire direction to $+x$ axis and broadside direction to z axis.

III. RESULTS

The simulations are carried out by CST Microwave Studio 2018. The pin diode employed is MA4AGP907 from MA-COM, which has a series resistance of $5.2\ \Omega$ and a capacitance of 0.025 pF. The reflection coefficient is represented in Fig. 2 for the two different states. The simulated -10 dB impedance bandwidth is 6 GHz (from 24 GHz to 30 GHz). For the frequency bands below 3 GHz, the matching criterion is more relaxed and set to -6 dB. The operating bandwidth of the PIFA antenna is 2680-2840 MHz. The total efficiency of the mm-wave array is 80 % and 86 % for the low-frequency antenna.

The radiation patterns of both configurations of the diodes are represented in Fig. 3. The $\phi = 0^\circ$ cut is plotted in Fig. 3 (a), it can be seen how the radiation pattern points to the endfire direction when the diodes are off, while the radiation is broadside when they are on. The maximum gain at 26 GHz

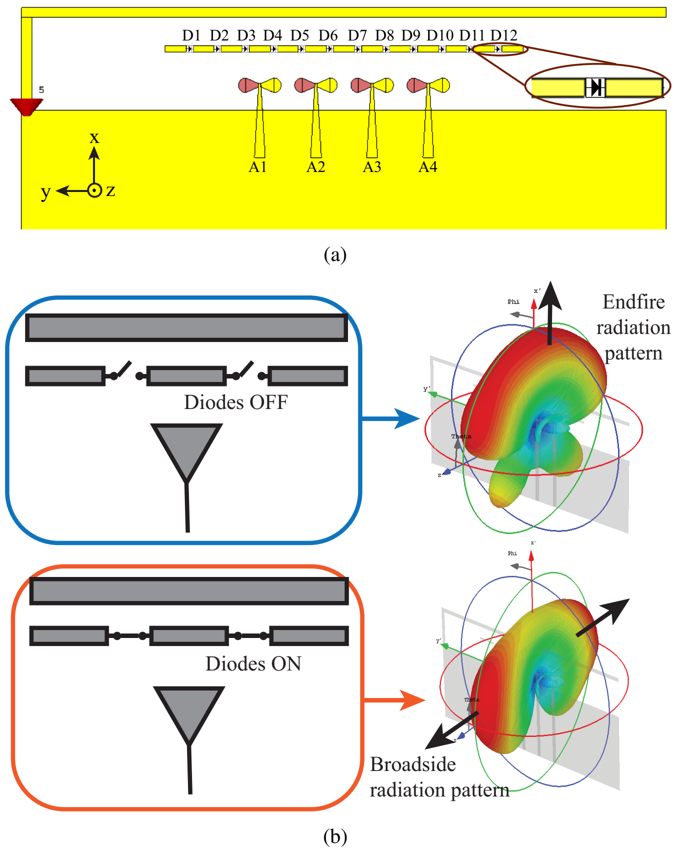

(a)

(b)

Fig. 1. (a) Simulated model of the structure. The substrate is hidden in this figure. (b) Functionality diagram.

for the endfire configuration is 8 dBi, while for the broadside radiation pattern it has a value of 9.2 dBi.

The beam-steering envelope is represented for several frequencies in Fig. 4. The envelope is obtained from the maximum gain of 12 beams pointing at different directions. The phase step between the antenna elements is 30°. In the case of endfire radiation pattern (Fig. 4 (a)), the beam is scanned in azimuth. While for broadside radiation pattern (Fig. 4 (b)), the scanned beam is represented in the YZ plane to plot the direction of maximum gain. The array is able to scan the beam $\phi = \pm 70°$ with an endfire radiation pattern. For the broadside radiation pattern, the scan angles are $\theta = \pm 42°$ and $\theta = 138°$-$223°$.

IV. CONCLUSION

A radiation pattern reconfigurable bow-tie array, that covers the mm-wave frequency bands n257 and n258 [1], is presented in this paper. The array is integrated with a low-frequency antenna to reduce the space occupied of the mobile terminal. Several diodes control the shape of the radiation pattern. When all the diodes are on, the power is radiated in the broadside direction; when they are off, in endfire. Both configurations of the radiation pattern are able to steer the beam, 140° for endfire and 84°, for broadside.

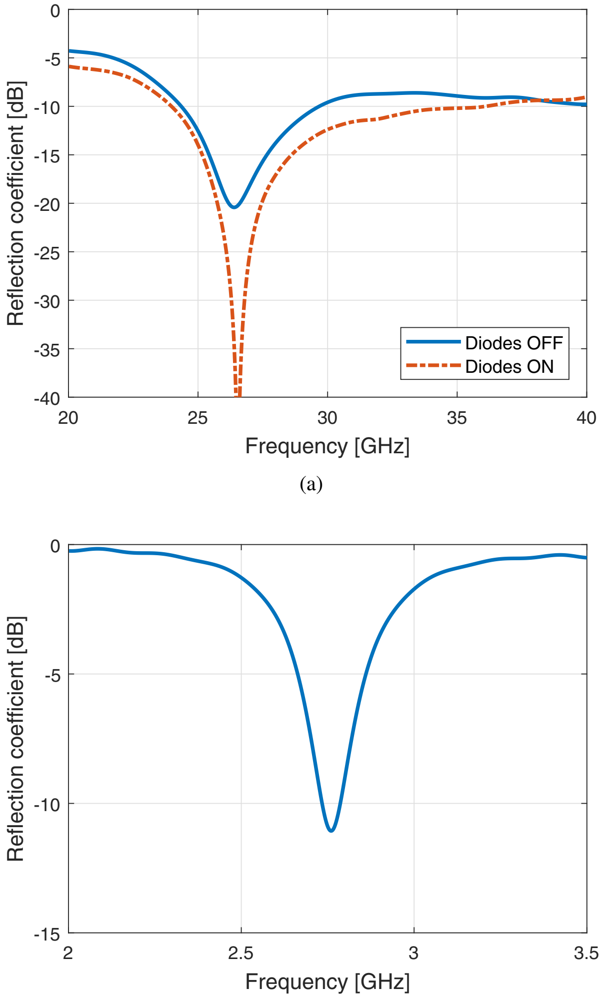

(a)

(b)

Fig. 2. (a) Reflection coefficient comparison of the two states of the mm-wave antenna. (b) Reflection coefficient of the PIFA antenna.

ACKNOWLEDGMENT

This work is supported by the InnovationsFonden project of RANGE (Reconfigurable Arrays for Next Generation Efficiency).

REFERENCES

[1] "General aspects for User Equipment (UE) Radio Frequency (RF) for NR (Release 15)," 3rd Generation Partnership Project (3GPP), Technical Report (TR) 38.817-1, 03 2019, version 15.3.0.

[2] T. S. Rappaport, S. Sun, R. Mayzus, H. Zhao, Y. Azar, K. Wang, G. N. Wong, J. K. Schulz, M. Samimi, and F. Gutierrez Jr, "Millimeter wave mobile communications for 5g cellular: It will work!" *IEEE access*, vol. 1, no. 1, pp. 335–349, 2013.

[3] W. Hong, K. Baek, Y. Lee, Y. Kim, and S. Ko, "Study and prototyping of practically large-scale mmwave antenna systems for 5g cellular devices," *IEEE Communications Magazine*, vol. 52, no. 9, pp. 63–69, Sep. 2014.

[4] R. Rodriguez-Cano, S. Zhang, K. Zhao, and G. F. Pedersen, "Reduction of main beam-blockage in an integrated 5g array with a metal-frame antenna," *IEEE Transactions on Antennas and Propagation*, vol. 67, no. 5, pp. 3161–3170, May 2019.

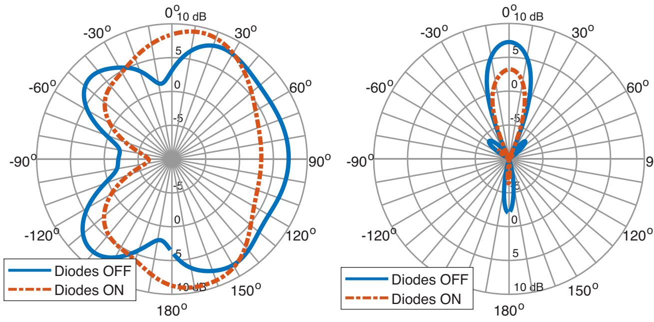

(a) (b)

Fig. 3. Realized gain radiation pattern cuts at 26 GHz. (a) $\phi = 0°$ cut. (b) $\theta = 90°$ cut. (See coordinate system in Fig. 1 (a)).

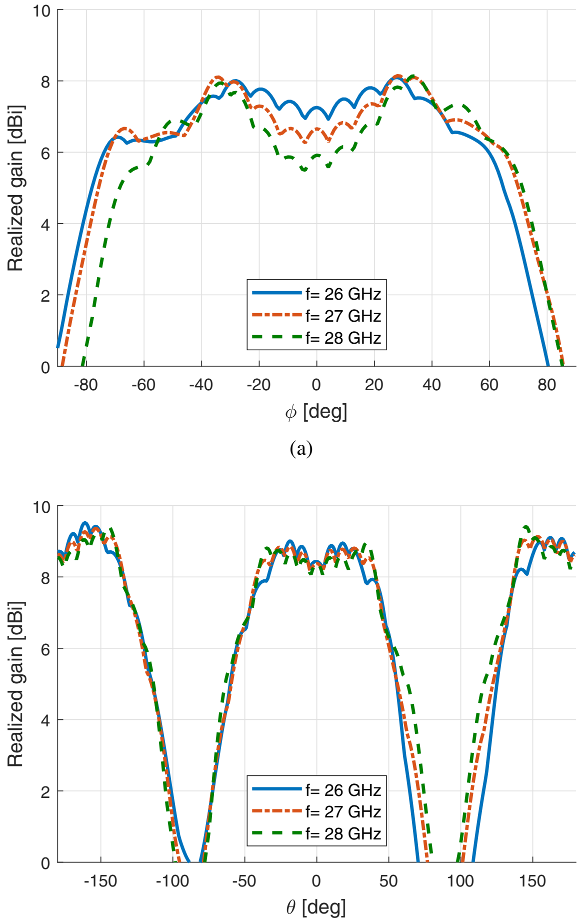

(a)

(b)

Fig. 4. Beam steering envelope comparison. (a) Diodes off ($\theta = 90°$ plane). (b) Diodes on ($\phi = 90°$ plane).

[5] J. Kurvinen, H. Kähkönen, A. Lehtovuori, J. Ala-Laurinaho, and V. Viikari, “Co-designed mm-wave and lte handset antennas,” *IEEE Transactions on Antennas and Propagation*, vol. 67, no. 3, pp. 1545–1553, March 2019.

[6] M. M. Samadi Taheri, A. Abdipour, S. Zhang, and G. F. Pedersen, “Integrated millimeter-wave wideband end-fire 5g beam steerable array and low-frequency 4g lte antenna in mobile terminals,” *IEEE Transactions on Vehicular Technology*, vol. 68, no. 4, pp. 4042–4046, April 2019.

[7] J. Zhang, S. Zhang, X. Lin, Y. Fan, and G. Pedersen, “3d radiation pattern reconfigurable phased array for transmission angle sensing in 5g mobile communication,” *Sensors*, vol. 18, no. 12, p. 4204, 2018.

[8] R. Santos, R. Penchel, M. Bontempo, and S. A. Cerqueira, “Reconfigurable printed antenna arrays for mm-wave applications,” in *Antennas and Propagation (EuCAP), 2016 10th European Conference on*. IEEE, 2016, pp. 1–5.